Basic Experiment on a Magnetoplasma Thruster Driven by Phase-Controlled RF

IEPC-2011-057

Presented at the 32nd International Electric Propulsion Conference,
Wiesbaden • Germany
September 11 – 15, 2011

Y. Yasaka[1], M. Yamamoto[2], Y. Hayashi[3], S. Nakamoto[4], H. Takeno[5] , and H. Yonemori[6]
Graduate School of Engineering, Kobe University,
Nada-ku, Kobe 657-8501, Japan

Abstract: Radio frequency (RF) driven magnetoplasma thruster is one of the electric propulsion systems, in which high density plasmas, produced by helicon wavelaunched from an RF system at a frequency $\omega / \Omega_i >> 1$ with Ω_i being the local ion cyclotron frequency, flow downward to the ion cyclotron range of frequencies heating section where the other RF system is used to excite ion cyclotron wave at $\omega / \Omega_i \sim 1$. Investigated is a new type of RF-driven magnetoplasma thruster with only one RF system for both plasma production and ion heating. This is accomplished with a pair of RF antenna windings forming the rotating field antenna. It is experimentally verified that for hydrogen plasmas the density of produced plasmas and the temperature of heated ions change sinusoidally with the phase difference peaking at $\pi/2$ and $-\pi/2$, respectively, showing the ability to control power ratio of the ion heating to the plasma production by only changing the phase difference. Design study of a dual-output variable-phase RF inverter is also performed for a future high-efficiency system component.

Nomenclature

A_m	=	spectral amplitude of mode number m of the antenna current
B_0	=	magnetic field strength at the throat, T
c	=	speed of light, m /s
D	=	$(R - L)/2$, the difference of the plasma dielectric components
$\boldsymbol{E}$	=	parallel (with suffix $\parallel$) and perpendicular ($\perp$) component of the electric field
E	=	energy of ions, J
I_{is}	=	ion saturation current
I_{sp}	=	specific impulse, s
I_θ	=	azimuthal component of the antenna current
k	=	parallel (with suffix $\parallel$) and perpendicular ($\perp$) component of wave number
L	=	plasma dielectric component for left hand polarization
M	=	mass of ions, kg
m	=	azimuthal mode number of RF
N	=	parallel (with suffix $\parallel$) and perpendicular ($\perp$) component of refractive index

[1] Professor, Department of Electrical and Electronic Engineering, yasaka@eedept.kobe-u.ac.jp.
[2] Graduate student, Department of Electrical and Electronic Engineering.
[3] Graduate student, Department of Electrical and Electronic Engineering..
[4] Research Associate, Department of Electrical and Electronic Engineering, nakamoto@eedept.kobe-u.ac.jp.
[5] Associate Professor, Department of Electrical and Electronic Engineering, takeno@eedept.kobe-u.ac.jp.
[6] Assistant Professor, Department of Electrical and Electronic Engineering, yonemori@eedept.kobe-u.ac.jp.

n_e	=	electron density, m^{-3}
P	=	plasma dielectric component for parallel direction
P_{RF}	=	net power of rotating RF, W
p	=	gas pressure, Torr
R	=	plasma dielectric component for right hand polarization
r	=	radius or radial direction, m
S	=	$(R + L)/2$, the sum of the plasma dielectric components
T_e	=	electron temperature, eV
t	=	time, s
V_r	=	retarding voltage of the Faraday cup, V
z	=	axial distance, cm
ϕ	=	phase difference of RF currents to the antenna, rad
κ	=	antenna coupling coefficient
θ	=	azimuthal angle or azimuthal direction, rad
Ω_σ	=	cyclotron frequency of species σ (= i for ion and e for electron)
ω	=	RF angular frequency
$\omega_{p\sigma}$	=	plasma frequency of species σ (= i for ion and e for electron)

I. Introduction

RADIO frequency (RF) driven magnetoplasma thruster is one of the electric propulsion systems, in which high density plasmas, produced by helicon wave (HW) launched from an RF system at a frequency $\omega / \Omega_i >> 1$ with Ω_i being the local ion cyclotron frequency, flow downward to the ion cyclotron range of frequencies (ICRF) heating section where the other RF system is used to excite ion cyclotron wave (ICW) at $\omega / \Omega_i \sim 1$. The ICRF waves resonantly interacts with ions and accelerate them in the direction perpendicular to the external magnetic field. A magnetic nozzle, which is a region where the magnetic field diverges, converts perpendicular velocity of ions into parallel velocity to create thrust [1,2]. The amounts of thrust or velocity of exhaust plasmas can be varied by controlling the RF powers in the two RF systems relatively or independently. RF inverters will be used for these RF systems because of their high efficiency, small footprint, and light weight.

We investigate a new type of RF-driven magnetoplasma thruster with only one RF system for both plasma production and ion heating. This is accomplished with a pair of RF antenna windings forming the rotating field antenna [3,4]. The windings are fed by two RF outputs with the same frequency at $\omega / \Omega_i \sim 1$ but with a relative phase difference. If the rotating field antenna excites left-rotating (azimuthal mode number $m = -1$) RF fields by proper phase control, the RF fields couple selectively to the $m = -1$ slow ICW, which accelerates ions at the ion cyclotron resonance. On the other hand, when the rotating field antenna generates right-rotating $m = +1$ fields, the fields excites the $m = +1$ fast wave, which is on the same branch as HW, resulting in acceleration of electrons and enhancement of ionization. Therefore, it is possible to control the power ratio of the ion heating to the plasma production by only changing the phase difference.

We also describe the design and circuit simulation of a two-phase RF inverter, to be used for the rotating RF system in future. It is thus demonstrated that the use of the rotating field for RF plasma production and ion heating provides novel controllability and technical prospect for the magnetoplasma thruster with a high-efficiency RF inverter.

II. ICRF Waves and Their Excitation

A. Wave Modes

We assume a cylindrical uniform cold plasma in a conducting cylinder immersed in a uniform static magnetic field along the axis. The wave field varies as $\exp[i(m\theta + k_\parallel z - \omega t)]$ propagating with the axial wavelength of $2\pi / k_\parallel$ and the azimuthal mode number m. The dispersion relation in terms of the perpendicular and parallel refractive indexes is given by

$$SN_\perp^4 - [PS + RL - N_\parallel^2 (P + S)]N_\perp^2 + P(R - N_\parallel^2)(L - N_\parallel^2) = 0, \quad (1)$$

where $N_\perp = k_\perp c/\omega$, $N_\parallel = k_\parallel c/\omega$, $S = \frac{1}{2}(R+L)$, $D = \frac{1}{2}(R-L)$, $R = 1-\sum_\sigma \frac{\omega_{p\sigma}^2}{\omega^2}(\frac{\omega}{\omega+\Omega_\sigma})$, $L = 1-\sum_\sigma \frac{\omega_{p\sigma}^2}{\omega^2}(\frac{\omega}{\omega-\Omega_\sigma})$, and $P = 1-\sum_\sigma \frac{\omega_{p\sigma}^2}{\omega^2}$. The boundary conditions at the conducting cylinder and in the vacuum layer between the plasma and the wall must be considered and are given in the literature [5]. As a result, the axial component of the wave electric field is given by

$$E_z = \sum_{\ell=1}^{2} A_\ell \mathrm{J}_m(k_{\perp\ell} r)\exp[i(m\theta + k_\parallel z - \omega t)], \tag{2}$$

where $k_\perp$ is obtained as solutions to Eq. (1) for a given $k_\parallel$, and the other components of the electric field are represented by Eq. (2) and other parameters.

Figure 1 shows the schematic dispersion relation of fast and slow waves of $m=+1$ and -1 modes in the frequency range near and above Ω_i (The $m = +1$ slow wave is not shown). Here, the $m=+1$ (-1) wave propagates in the sense of right-hand (left-hand) rotation with respect to the static magnetic field as seen by Eq. (2), and the electric field of the $m=+1$ (-1) wave has the right-hand (left-hand) circular polarization near axis, which is confirmed by examining the explicit expression for the perpendicular components of the electric field. The waves with frequencies $\omega/\Omega_i \gg 1$ are called as HWs. In the variable specific impulse magnetoplasma rocket (VASIMR) [2] or similar type ones, the $m = +1$ fast wave at $\omega / \Omega_i >> 1$ (HW) is used to accelerate electrons and produce high-density plasmas, and $m = -1$ slow wave at $\omega / \Omega_i \leq 1$ (ion cyclotron wave) is used to heat ions. Excitation of these waves is accomplished, so far, by using antennas with twisted current segments, which correspond to right or left-rotating propagation. The right-twisted antenna is for HW excitation and the left-twisted antenna for the ion cyclotron wave excitation. In this case, if the lengths of the two antennas are of the same order, the excited waves have the same values of $k_\parallel$ as shown by the vertical long line in Fig. 1, and two antennas must be driven at different frequencies as shown by the two horizontal arrows. Furthermore, the excited waves have proper polarizations only for one propagation direction and only in a very narrow range of $k_\parallel$ that is given by the pitch of the helix of the antennas.

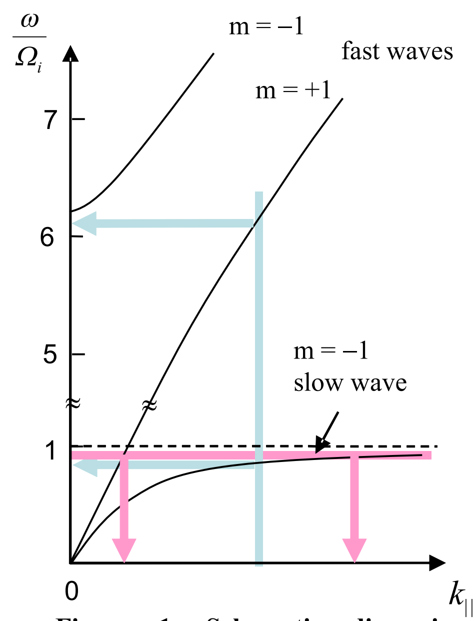

Figure 1. Schematic dispersion relation of the fast and slow waves of m = +1 and –1 modes in ICRF.

On the other hand, when the driving frequencies of the two antennas are set to the same value as shown by the long horizontal line in Fig. 2, the antenna for the m = +1 wave excitation should excite small $k_\parallel$ component and the other antenna for the m = −1 wave excitation should excite large $k_\parallel$ component as shown by the two vertical arrows. If an antenna with wide $k_\parallel$ spectrum is used, it can excite both the m = +1 and −1 waves achieving plasma production and ion heating at one location. Since the antenna excites many $k_\parallel$ components, the antenna-plasma coupling is not much affected by changes of the dispersion relation caused by changes in plasma density or magnetic field. We will describe such a new type antenna in the next section.

B. Rotating Field Antenna

We employ the rotating field antenna shown in Fig. 2(a) in order to select the m number of the excited RF field. The antenna consists of two windings aligned axially and displaced by 90° with each other in the azimuthal direction. The windings are driven by RF currents with variable phase difference of ϕ. By adjusting the phase difference to $\pi/2$ or $-\pi/2$, we can establish the RF field to rotate in the right or left azimuthal direction. This can be understood by Fig. 2(b) where the power spectrum amplitude of the azimuthal antenna current distribution $I_\theta(\theta)$ is plotted versus m using the relation;

$$A_m = \frac{1}{2\pi}\int_0^{2\pi} I_\theta(\theta)\exp(-im\theta)\, d\theta\,. \tag{3}$$

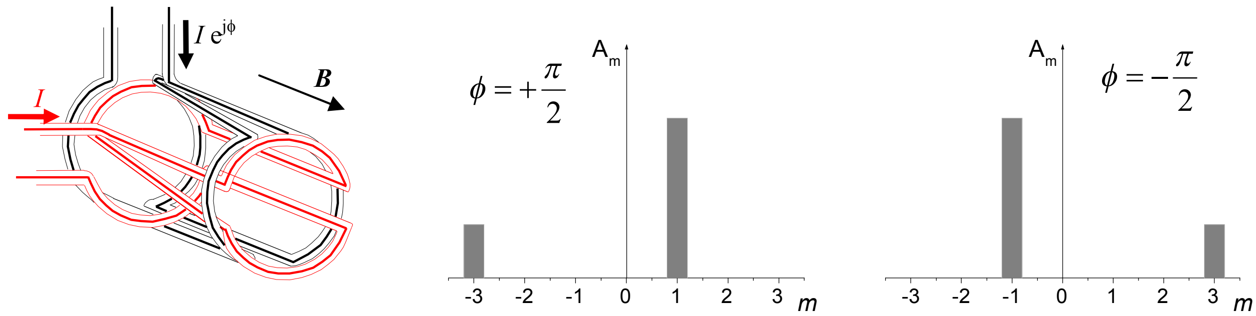

Figue 2. (a) Configuration of the rotating field antenna. (b) Comparison of the power spectrum of the azimuthal mode for the currents of the rotating field antenna with $\phi = +\pi/2$ and $\phi = -\pi/2$.

By choosing the phase difference of the currents in two windings, the antenna can selectively excite the $m = +1$ right hand rotating mode or the $m = -1$ left hand rotating mode. It is therefore possible to vary the ratio of the amplitude of $m = +1$ mode to $m = -1$ mode. The axial mode number $k_{\|}$ is unaffected by the variation of ϕ , and has a broad spectrum since the windings are not twisted.

C. 2D Calculation of Wave Propagation

We use a 2-dimensional fluid simulation code [6] to obtain wave fields and power absorption in a nonuniform plasma immersed in nonuniform magnetic fields. The simulation code numerically analyzes the plasma maintained by global electric fields via wave propagation. The code repeatedly calculates wave propagations, plasma transports, and gas phase chemical reactions after loading external input files of configuration setting, parameters, initial condition and cross section data. The storage spaces are given to all parameters necessary for the calculation, and the parameters in storage spaces are successively updated in each calculation. The finite element method is used for the calculation of the global electric field ***E*** via wave propagation, which is given by

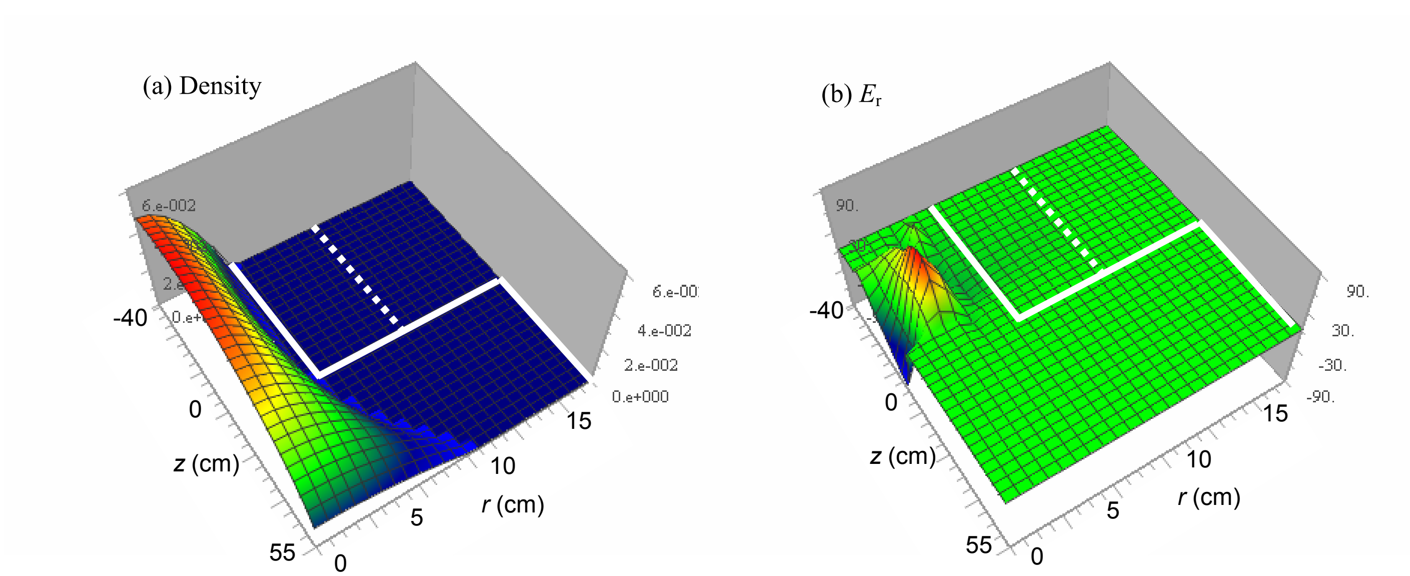

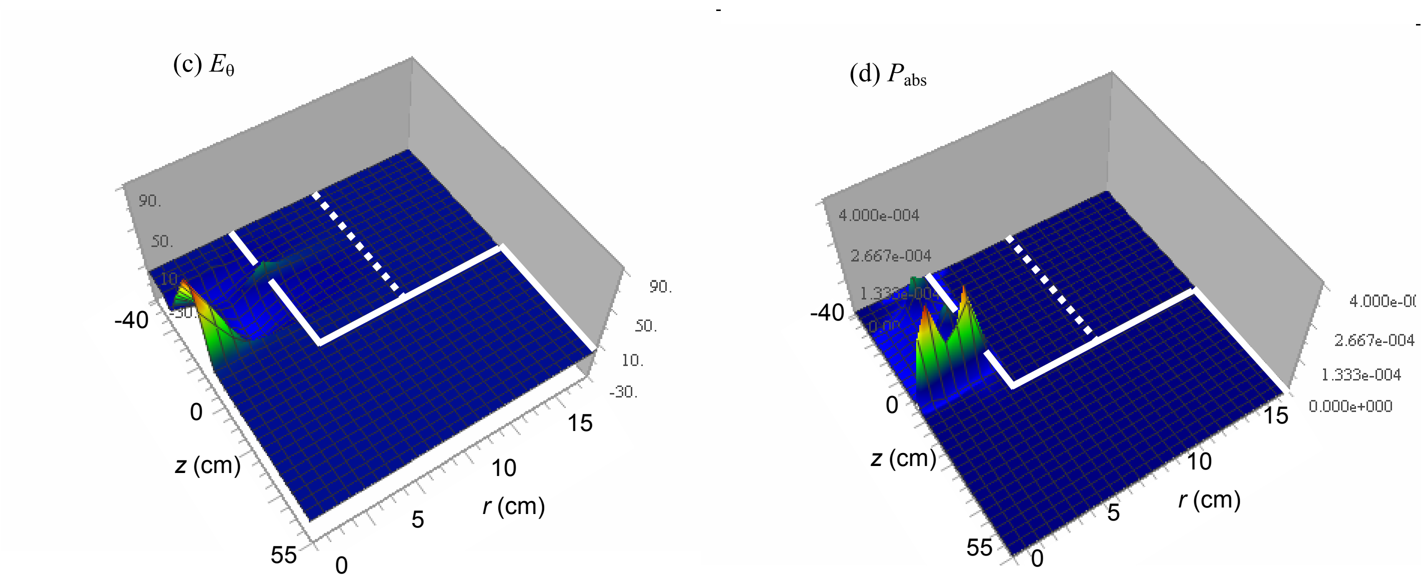

Figue 3. (a) Assumed density profile and calculated profiles of (b) radial component of the electric field E_r, (c) azimuthal component of the electric field E_θ, and (d) absorbed power P_{abs}. Thick lines in each figure show the boundary of the chamber and dotted line shows a metallic sheild.

$$\nabla \times \nabla \times \boldsymbol{E} - \omega^2 \mu_0 \varepsilon_0 \overleftrightarrow{\varepsilon}\, \boldsymbol{E} = i\omega\mu_0 \boldsymbol{J}_{ext}\,, \tag{4}$$

where ω, μ_0, ε_0, $\overleftrightarrow{\varepsilon}$, and Jext are the frequency of the wave, permeability, permittivity in vacuum, dielectric tensor, and the external RF current (power source), respectively. The power absorption P_{abs} of electrons from the wave field is calculated using

$$p_{abs} = \frac{1}{4} i\omega\varepsilon_0 \boldsymbol{E}^* \cdot \left(\overleftrightarrow{\varepsilon}^{*T} - \overleftrightarrow{\varepsilon} \right) \cdot \boldsymbol{E}, \tag{5}$$

where * is the complex conjugate, and T is the transposition.

In performing calculation, we assume the same configuration as the experiment; a glass tube of 5-cm in radius and 40-cm long attached to a metal chamber of 17.5-cm in radius and 55-cm long. The rotating field antenna is represented by a current segment with the azimuthal variation of m = +1 or m = −1 mode. A divergent magnetic field is applied with a maximum value of 1.45 kG and an effective mirror ratio of 10. Figure 3 shows (a) assumed density profile of $n_e = 5 \times 10^{18}\,\mathrm{m}^{-3}$ (hydrogen ions) and calculated profiles of (b) radial component of the electric field E_r, (c) azimuthal component of the electric field E_θ, and (d) absorbed power P_{abs}. Thick lines in each figure show the boundary of the chamber and dotted line shows a metallic sheild. Electric fields excited from the antenna at z = −32 cm propagate downstream forming the azimuthal mode of m = −1 and with radial variation having a node at $r \sim 1.5$ cm for E_r and 2.5 cm for E_θ as shown in Figs. 3 (b) and (c), respectively. A small peak in E_θ at $r \sim 5$ cm is just the antenna field. As the wave approaches to the axial position of $z \sim 0$, where $\omega / \Omega_i = 1$, amplitudes of E are strongly damped and power absorption arises locally as shown in Fig. 3 (d).

III. Experiment on Magnetoplasma Thruster

A. Device

The experimental device for the RF-driven magnetoplasma thruster is schematically shown in Fig. 4. We employ the rotating field antenna driven at $\omega / 2\pi$ = 1.9 MHz in order to select the m number of the excited RF field. The antenna consists of two dual-double-half-turn like windings aligned axially and displaced by 90° with each other in the azimuthal direction. The windings are driven by RF currents with a variable phase difference of ϕ. By adjusting the phase difference to +π/2 or −π/2, we can establish the RF field to rotate in the right (m = +1) or left (m = −1) azimuthal direction. It is therefore possible to vary the ratio of the amplitude of the m = +1 mode to the m = −1 mode. At present, we use two RF linear amplifiers instead of the two-output RF inverter. The magnetic field strength is B_0 = 1.7 kG at maximum, and the feeding propellant is hydrogen. The additional antenna driven by a base RF at 13.56 MHz is used to break down the gas and initiate the plasma. The right end of the device shown in Fig. 4 is attached to the magnetic nozzle and a vacuum chamber.

The plasma starts by applying the base RF of < 1 kW with the gas feed at pressures of 10-20 mTorr. Then the rotating RF antenna is powered by two class-C amplifiers excited by a signal generator of 2-output with variable phase difference. The amplifiers may be replaced by a two-phase inverter in future. The rotating RF is applied for a time duration of ~ 2 ms with a duty ratio of ~ 10%. The density or the ion temperature increases depending on the phase difference of the currents to the rotating field antenna. When the right-rotating excitation is used, the m = +1 fast wave is preferentially launched. The m = +1 fast wave, which is right circularly polarized, does not couple with ions which gyrate in the left-hand sense, and rather couple with electrons at large axial (parallel) velocities to enhance ionization. For left-rotating excitation, ions are selectively accelerated at the ion cyclotron resonance (B_0 = 1.25 kG for hydrogen ions) located at -10 cm < z < 0. The heated plasma enters into a magnetic nozzle at 10 < z < 50 cm to transform perpendicular energy into parallel energy.

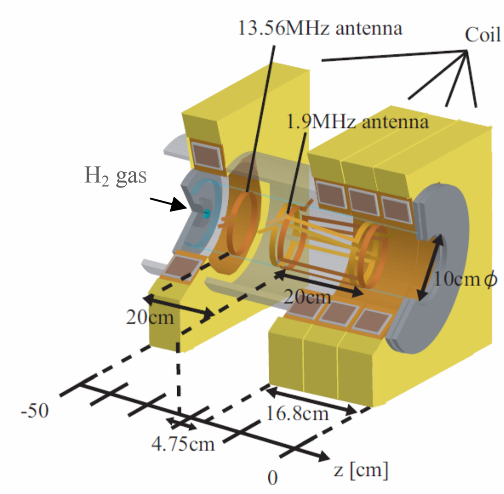

Figure 4. Configuration of the RF-driven magnetoplasma thruster.

B. Plasma Production and Heating

Figure 5(a) shows the ratio of the increment of ion saturation current I_{is} to the base value that is produced by the base RF as a function of the RF power P_{RF} of the one winding of the rotating field antenna for helium plasma with

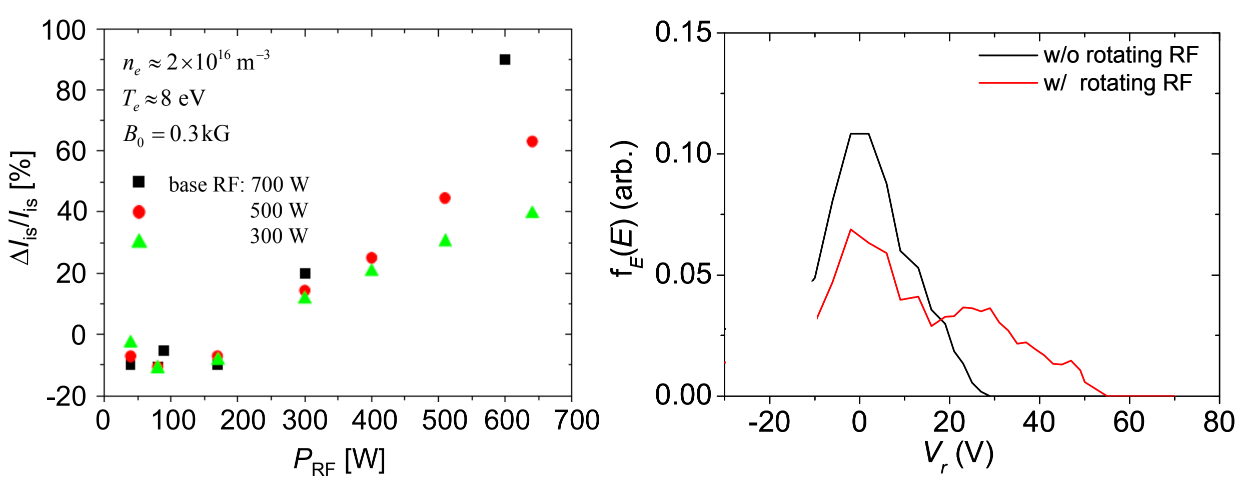

Figure 5. (a) Ratio of the incremental ion saturation current to the base value as a function of P_{RF} for three cases of base RF power, and (b) energy distribution function of ions after the magnetic nozzle with and without P_{RF}.

base parameters measured at z = 40 cm; plasma density $n_e = 2.0\times10^{16}$ m^{-3}, electron temperature $T_e = 8$ eV, B_0 = 0.3 kG at the throat, and the gas pressure p = 20 mTorr. It is shown that, while I_{is} rather decreases for very small values of P_{RF}, I_{is} increases proportionally to P_{RF} reaching 50-100 % increase relative to the base value. Since there is no cyclotron resonance in this case, the ion temperature does not change.

We use hydrogen gas and higher magnetic field of B_0 = 1.3 kG to set the ion cyclotron resonance under the rotating field antenna. The voltage-current characteristics are obtained by using the Faraday cup aligned axially at a position of z = 50 cm, after the magnetic nozzle. Figure 2(b) shows the energy distribution function of ions f_E for P_{RF} = 1.0 + 1.0 kW (1.0 kW for each winding of the rotating field antenna) with no phase difference. The abscissa is the retarding voltage V_r applied on the collector of the Faraday cup with a voltage of − 110 V on the electron suppressor grid. The values of f_E for $V_r < -10$ V are not plotted since the *V-I* characteristics do not saturate for large negative values of V_r due to secondary electron emissions and ion acceleration for this type of electrode configuration. We note that hydrogen ions are strongly accelerated and heated with the application of the rotating RF due to the ion cyclotron resonance and that their energy is converted from perpendicular to parallel direction with respect to the magnetic field after passing through the magnetic nozzle.

C. Application of the Phase-Controlled RF

We now operate the rotating field antenna feeding the RF currents with variable phase difference to the two windings. The phase difference is monitored at the directional coupler connected between the RF amplifier and the matching circuit for each winding.

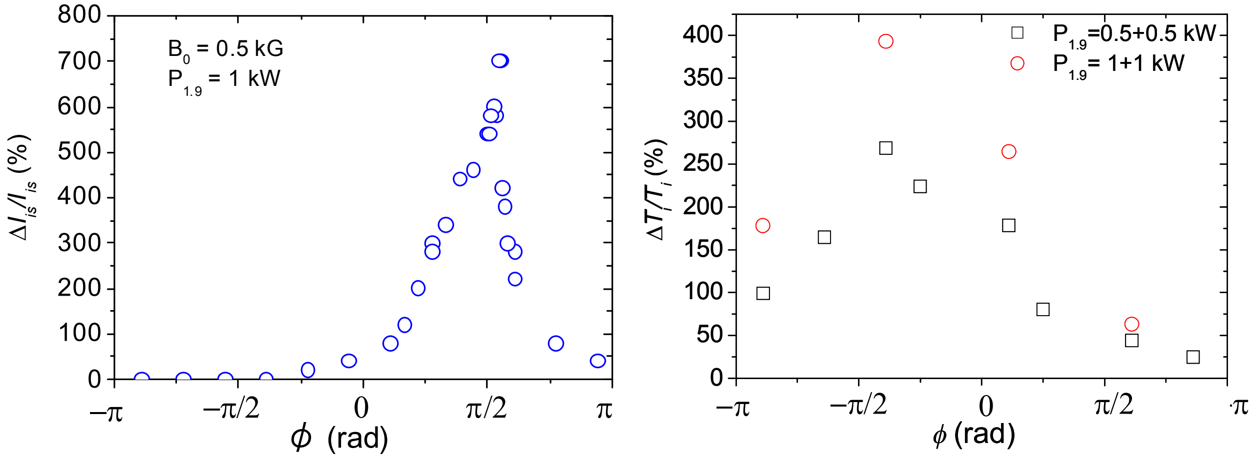

Figure 6 (a) Incremental ion saturation current and (b) incremental ion temperature as a function of the phase difference. Both incremental values are normalized to the initial values.

The increment of I_{is} over the value that is produced by the base RF normalized to the initial value is plotted versus the phase difference in Fig. 6(a) for P_{RF} = 0.5+0.5 kW into the base hydrogen plasma of $n_e = 3.7\times10^{16}$ m^{-3}, $T_e = 10$ eV, and B_0 = 0.5 kG. The Langmuir probe was located at z = 40 cm. It is clearly seen that strong plasma production takes place in a limited region of ϕ near $90^\circ (= +\pi/2)$, where the rotating field antenna excites right-rotating $m = +1$ fields that are expected to couple selectively to the $m = +1$ fast wave, which accelerates electrons and enhances ionization.

Figure 6(b) is the normalized increment of the ion temperature as a function of ϕ for hydrogen plasma with B_0 = 1.5 kG for two values of P_{RF} ; 0.5+0.5 kW (rectangular symbols) and 1.0 +1.0 kW (circular symbols) as measured by the Faraday cup located at z = 50 cm. In this case, contrary to Fig. 6(a), the maximum increase in T_i takes place around ϕ = $-90^\circ (= -\pi/2)$, where the rotating field antenna excites left-rotating $m = -1$ RF fields that are expected to couple selectively to the $m = -1$ slow wave, which accelerates ions at the ion cyclotron resonance. Figures 6(a) and (b) indicate that the plasma production or ion heating varies nearly sinusoidally with ϕ , but with the displacement of π.

By using the data points for P_{RF} = 1.0 +1.0 kW in Fig. 6(b), the value of the exhaust velocity of ions v_{ex} is calculated from the average energy E to be $\sqrt{2E/M}$, with M being the ion (hydrogen) mass, and plotted in Fig. 7 as a function of ϕ. The value of v_{ex} is maximum at a phase of −π/2. If the supplied gas is almost fully converted to the plasma, the specific impulse I_{sp} is estimated to be $\sim v_{ex}/g$, with g being the acceleration of the gravity. It is thus possible to vary v_{ex} by only changing the phase difference between the RF currents in the two windings of the rotating field antenna without the necessity to change the RF power or other conditions. It is noted in previous works [1,2] that two power sources are necessary for plasma production and heating and the control of the plasma density and ion temperature requires adjustment of the output powers of the two power sources. Figures 6 and 7 demonstrates that the use of the rotating field antenna enables one to perform a novel control of the plasma density and ion temperature by the phase difference not by the powers for production and heating. It should also be noted that RF inverters, which may be employed in practical use of this type of thrusters, work with best efficiencies at a rated power. The efficiency degrades for lower output powers and no adjustment of the output power level is preferable.

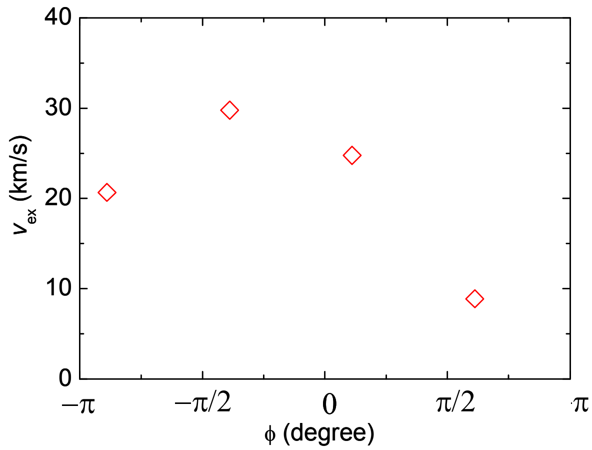

Figure 7. Exhaust velocity of ions relative to that of the base plasma as a function of ϕ of the rotaitng RF.

IV. Design of RF Inverter for the Phase-Controlled RF System

In the previous sections we described the experimental results using the rotating field antenna with two class-C RF amplifiers. In near future, use of inverters will significantly improve power efficiency or compactness of the system. We are considering to construct a dual-output variable-phase inverter operating at 1.9 MHz as shown in Fig. 8.

Two arms (Q1-Q2, Q3-Q4) are switched alternatively with a phase difference to provide RF powers P_1 and P_2 to the loads of antenna windings (Lp1-Rz1, Lp2-Rz2). Rz is divided into the vacuum resistance of the winding and effective plasma loading. Two FET's at each arm are switched on and off with a duty of 50 % at 1.9 MHz with resonant LC circuit (Lr1-Cr1, Lr2-Cr2) working as a waveform shaper. We designed two kinds of circuits; one is without the phase shift network indicated by the dotted rectangle (PS), and the other is with PS. In the case without PS, Cs1 is open and Cs2 is short-circuited. Cms's and Cmp's are for impedance matching. The antenna windings, shown in Fig. 2(a), are orthogonal with each other, but have a small mutual inductance between Lp1 and Lp2 represented by the antenna coupling coefficient κ.

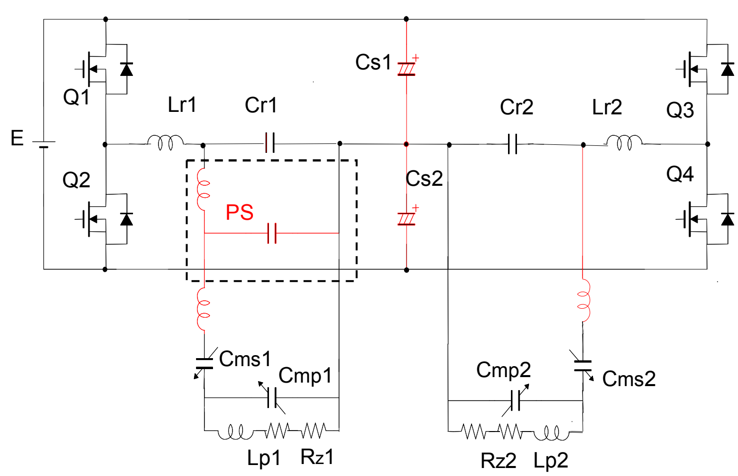

Figure 8. Circuit diagram of the dual-output variable-phase inverter.

We perform circuit simulation assuming a 1-kW class FET for each Q. The coupling between two antennas affect the operation of the inverter, and the phase difference and output powers change from those of initial setting. When the phase difference of the two outputs is initially set to 90°, it deviates to larger values due to the mutual coupling of Lp1 and Lp2 for the circuit without PS. By using PS, the deviation is suppressed as shown by the dotted line in Fig. 9. Similarly, unbalance of the powers delivered to Rz1 and Rz2 can be compensated by the control. At present, the amount of the power decreases with increased antenna coupling. It is expected that the rotating field antenna can be driven by one RF inverter as shown in Fig. 9 realizing small footprint, and light weight power source.

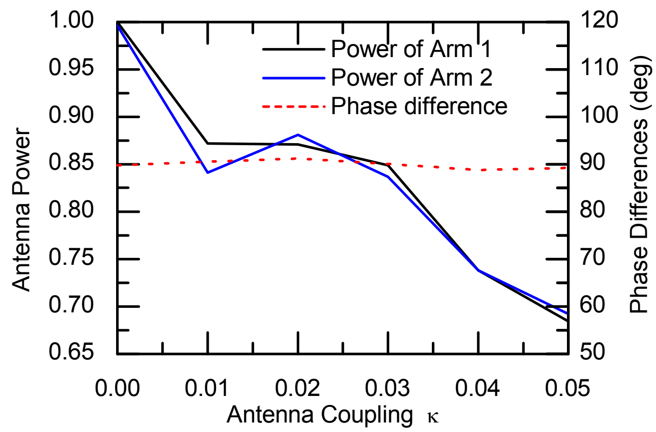

Figue 9. The deviation of the phase difference of the two outputs as a function of the coupling coefficient.

V. Summary

It is demonstrated that the rotating field antenna provides a novel control of the plasma density and ion temperature by the phase difference not by the powers for production and heating. This characteristics are very much suitable to RF inverters, which may be employed in practical use of this type of thrusters, because they exhibit best efficiencies at a rated power and the efficiency degrades when changing output power levels.

Design study of a dual-output variable-phase RF inverter has been performed. The mutual coupling between the loads, i.e., two windings of the rotating field antenna, affects the phase and amplitude of outputs of the inverter to deviate from a setting. The effects can be minimized by employing the additional circuit and control method.

Acknowledgments

The authors would like to thank Mrs. S. Nishino and H. Wakabayashi for the technical assistance in the experiments, and Mr. M. Nishidzu for the help of the circuit simulation.

References

[1] Chang-Diaz, F., and Squire, J., "The VASIMR Engine: Project Status and Recent Accomplishments," *AIAA Aerospace Sciences Meeting and Exhibit*, AIAA, Nevada, 2004, 0149.

[2] Bering, E., Chang-Diaz, F., Squire, J., Glover, T., Carter, M., McCaskill, G., Longmier, B., Brukardt, M., Chancery, W., and Jacobson, V., "Observations of Single-Pass Ion Cyclotron Heating in a Trans-Sonic Flowing Plasma," *Phys Plasmas*, Vol. 17, 2010, 043509.

[3] Yasaka, Y., and Itatani, R., "Direct Comparison between Circularly and Linearly Polarized RF Fields in ICRF Heating," *Nucl. Fusion,* Vol. 20, 1980, 1391.

[4] Yasaka, Y., Majeski, R., Browning, J., and Hershkowitz, N., "ICRF Heating with Mode Control Provided by a Rotating Field Antenna," *Nucl. Fusion*, Vol. 28, 1988, 1765.

[5] Allis, W., Buchsbaum, S., and Bers, A., *Waves in Anisotropic Plasmas*, MIT Press, Cambridge, 1963.

[6] Yasaka, Y. and Hara, Y., "Role of Helicon Waves on High-Density Plasma Production," *Jpn. J. Appl. Phys*., Vol. 33, 1994, pp. 5950-5958.